Int. J. Heat Mass Transfer. Vol. 19, pp. 471–478. Pergamon Press 1976. Printed in Great Britain

HEAT AND MASS TRANSPORT ACROSS DIFFUSIVE INTERFACES BOUNDED BY TURBULENT CONVECTING REGIONS

R. A. WIRTZ* and C. S. REDDY†
Mechanical and Industrial Engineering Department, Clarkson College of Technology, Potsdam, NY 13676, U.S.A.

(*Received* 28 *January* 1975 *and in revised form* 18 *August* 1975)

Abstract—The vertical transport of heat and solute across a stable diffusive interface separating two turbulent convecting regions of different concentration is experimentally investigated. Convection in this case is driven by sideways heating such that the horizontal interface separating the convecting regions is sandwiched between two opposite flowing turbulent boundary layers. Flux laws, for the vertical heat and solute transport are developed. These laws are then used to study the effect of changes in layer size and number on vertical transport in multilayered convecting systems. It is found that the vertical transport in such systems is independent of convecting layer size or number.

NOMENCLATURE

B, Brunt–Väisälä frequency;
c, fluid specific heat;
C_1, C_2, C_3, empirical constants;
D_S, solute diffusivity;
D_T, heat diffusivity;
F_S, vertical flux of solute;
F_T, vertical flux of heat;
F_w, wall heat flux;
g, gravitational acceleration;
h, convective layer thickness;
$\bar{h}$, length scale in layered system;
H, region height in layered system;
L, thickness of diffusive interface;
Le, fluid Lewis number;
N, number of diffusive interfaces in layered system of height H;
Nu_w, wall Nusselt number;
r, solute resistance [see equation (17)];
R, Rayleigh number for stratified system;
Ra, Rayleigh number for homogeneous system;
R_ρ, stability number;
S, solute weight fraction;
$\bar{S}$, mean solute weight fraction;
T, fluid temperature;
$\bar{T}$, mean fluid temperature;
W, width of region;
z, vertical coordinate.

Greek symbols

α, coefficient of thermal expansion;
β, coefficient of expansion due to solute;
ΔS_0, salinity difference between convecting regions;
ΔS_l, salinity change in boundary region;
ΔS_L, salinity change in diffusive region;
ΔT_w, wall temperature difference;
ΔT_l, temperature change in boundary region;
ΔT_0, temperature difference between convecting regions;
ρ, fluid density;
$\bar{\rho}$, mean fluid density;
ν, fluid kinematic viscosity.

1. INTRODUCTION

WE ARE interested in experimentally investigating the vertical transport of heat and salt across a diffusive interface separating two turbulent convecting regions of different solute concentrations. The arrangement of solute concentrations, aqueous salt solutions in the present investigation, is such as to produce a step-like, kinematically stable density distribution. The convection in the regions above and below the diffusive interface is driven by sideways heating of the fluid, so that the turbulent convection adjacent to the diffusive region has some mean lateral motion superimposed upon it. This general arrangement is shown schematically in Fig. 1, where the flow in each convecting region is clockwise.

The interaction of convective layers, separated by diffusive interfaces, is a subset of a general class of two-component diffusion phenomena whose common characteristic is a difference in the magnitude of the species diffusivities (in this case heat and salt) which gives rise to the transport phenomena observed. Perhaps the best known example of this is when the component with smaller diffusivity is destabilizing, resulting in the so called "salt finger" instability. Turner [1] has recently reviewed various two-component mechanisms.

In the present investigation we are interested in the "diffusive" mechanism in two-component diffusion. That is, our primary flow arrangement is such that the species with smaller diffusivity (salt) is stabilizing.

*Assistant Professor.
†Research Assistant.

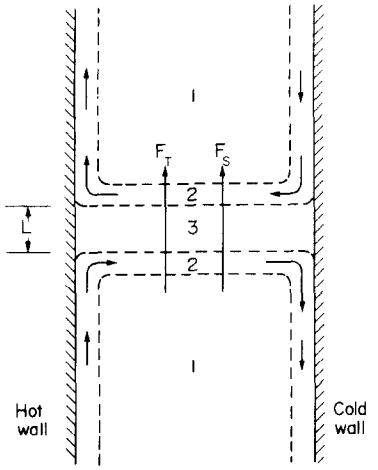

FIG. 1. Schematic of laterally heated convecting regions separated by a diffusive interface of thickness L. Turbulent convection is in boundary and mixed region (2 & 1) and is driven by side wall heating. Vertical fluxes of heat, F_T, and solute, F_S, are due to temperature and solute concentration differences across the diffusive region (3).

Vertical transport across a diffusive interface has previously been studied experimentally by Turner [2], and more recently Mancini *et al.* [3]. Their findings indicated that the ratio of solute flux to heat flux, F_S/F_T in Fig. 1, was constant under sufficiently strong stratification. Our investigation is different from theirs in that they investigated the case of pure heating from below resulting in turbulence with no mean lateral motion whereas in our experiments turbulent fluid motion adjacent to the diffusive interface is horizontal.

Circulating convective layers separated by diffusive interfaces occur when a continuously stratified fluid is heated laterally. Upon sufficiently strong heating, equisized layers form spontaneously, and grow laterally. The stability limits for such layer formation has been studied experimentally [4, 5], numerically [6, 7] and through linear theory [4, 8, 9]. Turner and Chen [10] have also recently studied convective layering formed by two-dimensional effects other than heating. One intriguing aspect of such flows is that the convective layers which are formed initially, merge two into one to form layers of double their original size as time progresses. This process repeats itself on a periodic basis, yet the layered system which always remains consists of approximately equisized convective layers. The results obtained in this study are used to investigate how the vertical flux of heat and salt is effected by this merging process.

Step-like structures in temperature and salinity have been observed in the Northeast Atlantic [11], the Arctic Ocean [12], Antartic Lakes [13], the Indian Ocean [14], near Bermuda [15], and at the bottom of the Red Sea [16]. Since layered systems produce significant departures in the vertical transport of heat and salt, an understanding of these processes is crucial in studying the local and global air–sea heat balance. Turner ([17] chapter 8), has discussed the oceanographical implications of layered systems. Hurle and Jackeman [18], have also identified layered convection processes in semi-conductor crystal growth operations. In this case, Soret effect diffusion is the double-diffusivity mechanism.

In Sections 2–4 we describe our experimental apparatus, operating procedures, and make some general observations about the nature of the convection processes under study. This is followed, in Section 5, by an analysis of data collected along the vertical centerline of our convection apparatus, leading to empirically based vertical flux laws. Assuming that transport in the diffusive interface region is essentially one dimensional we extend these results to consideration of multilayered convecting systems in Section 6 where we find that the vertical solute flux in a multilayered system is independent of the number, or size, of the layers existing at a given time.

2. APPARATUS

The test region, which is shown schematically in Fig. 2, consisted of a 290 mm high × 146 mm wide × 125 mm deep rectangular enclosure. The two sides of the enclosure parallel to the page were made of $\frac{1}{4}$ in (6.3 mm) thick plate glass for viewing; the bottom consisted of $\frac{1}{2}$ in (13 mm) thick epoxy painted wood and a glass cover was fitted to the top. The remaining two vertical sides consisted of $\frac{1}{8}$ in (3.2 mm) thick aluminium plates backed with circulating passages. Copper–constantan thermocouples were attached to the rear of each surface exposed to the circulating water. All thermocouples were wired in differential fashion relative to the cold wall and the copper leads were run through a copper thermocouple switch to an integrating DVM with a sensitivity of $\pm 1\,\mu$V. We estimate temperature difference measurements to be accurate to within ± 0.1°C. The aluminum plates were determined to be isothermal to within $\pm 3\%$ and we estimate that the wall temperature difference could be maintained constant to within ± 0.5°C.

A traverse mounted probe was placed along the

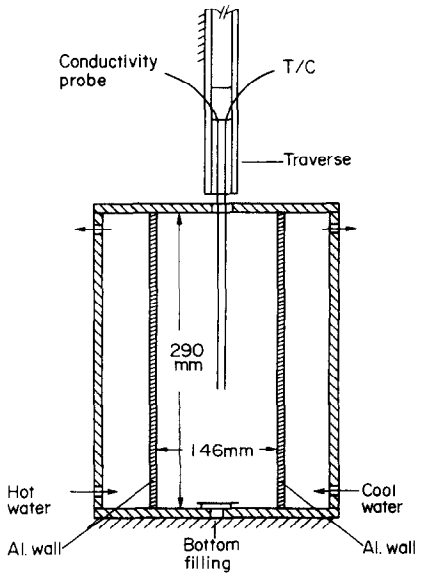

FIG. 2. The test apparatus used in the present investigation.

vertical centerline of the tank. It could be positioned to within ±0.02 mm. The probe consisted of a 30 gage (B & S) copper–constantan thermocouple mounted in a 1.6 mm O.D. ceramic tube adjacent to a 0.8 mm O.D. thin wall stainless steel tube which acted as a siphon for the withdrawal of solution samples. The thermocouple bead, a gas welded junction, was exposed, yet electrically insulated from the fluid with a varnish coating. The siphon tip located at the same level, but approximately 5 mm to the side of the thermocouple bead had a 30° acute angle bevel to form a sharp point. This slender point was then folded over in "L" fashion. This insured that the sample withdrawn could only enter the siphon laterally.

The other end of the stainless steel tube was connected, via a short length of surgical tubing to a Beckman Pipette conductivity cell. Small samples (≈ 1 ml volume) were drawn into the conductivity cell and their salinity was output on a Beckman Type RA5 temperature compensated conductivity meter. The samples were discarded after analysis. The calibration of the conductivity apparatus was checked against standard solutions before and after each experiment. We estimate our conductivity apparatus to be accurate to within ±0.1 wt % salt with a spatial resolution radius of approximately 3 mm.

3. PROCEDURE

The apparatus was filled in step fashion with two salt solutions. The solutions were lightly stirred to sharpen the salinity interface between convecting regions and to insure that the convecting regions were at uniform salinity. When the fluids were again quiescent, the circulating passages were opened to allow the isothermal walls to reach their desired temperature difference.

Convection commenced immediately in the homogeneous regions. The vertical flow along the isothermal wall approached the diffusive interface and then, upon reaching it turned laterally. For the data reported on here we have not observed any penetration through the diffusive interface of the vertical flow near the side walls. At the start of the experiment the diffusive interface nearest the isothermal wall was displaced vertically on the order of 2–3 mm. This vertical displacement propagated out from the wall as the convection stabilized, until after between 0.5 and 1.5 h the diffusive region was straight and at approximately 1–2° from the horizontal, the angle depending on the imposed wall temperature difference.

The thickness of the diffusive region depended on the imposed wall temperature difference and the salinity difference between convecting regions. Since vertical transport in this region is by diffusion, it was necessary to wait at least one characteristic diffusion time before assuming that the transport processes were quasi-steady. We estimated this waiting time as $(L/2)^2/D_S$ where L is the expected interface thickness and D_S is the salt diffusivity ($= 1.5 \times 10^{-5}$ cm^2/s). This results in waiting times between 4.6 and 42 h for interface thickness between 1 and 3 cm.

4. GENERAL OBSERVATIONS

The flow situation observed at quasi-steady conditions is shown schematically in Fig. 1 based on our shadow and schlieren observations. It consists of a diffusive interface region (No. 3) a few cm thick bounded above and below by two convecting regions, which we further subdivided into a mixed region (No. 1) and a boundary layer region (No. 2). The mixed regions are quiescent with homogeneous salinity and almost linearly stable temperature stratification in the vertical. This results in a weak salt finger structure which may be observed with a vertical knife edge schlieren. We have found that horizontal variations of temperature and salinity are small within the mixed region.

The flow driven by the wall temperature difference is confined to a turbulent boundary layer which forms adjacent to the isothermal walls and above and below the diffusive region. Both salinity and temperature vary in a nonlinear fashion here. The mean flow in the turbulent boundary is parallel to the diffusive interface. A small thermocouple (0.075 mm O.D. wire) placed in the midheight of the horizontal boundary measures a regular temperature fluctuation of approximately 0.4°C amplitude and 10–15 s period. Our schlieren images (using a pinhole aperture or a vertical knife edge) indicate a regular spire-like pattern which develops as the fluid is convected across the tank. The pattern develops faster with larger imposed wall temperature difference. We have not been able to produce clear schlieren images of these spires. This may indicate that the patterns represent a three dimensional secondary flow. We have concentrated on measurement of mean quantities in this work.

Sandwiched between the almost horizontal boundary layers is an essentially quiescent region with linear temperature and salinity gradients. This diffusive region is of uniform thickness inclined at about 1–2° to the horizontal across the tank, with a slight thickening near the isothermal walls.

Representative temperature and salinity profiles measured along the verticle centerline of the tank are plotted in Fig. 3 showing the homogeneous salinity mixed region, the boundary layer region, and the diffusive region with linear temperature and salinity gradients.

Figure 4 shows the variation in temperature and salinity within the diffusive interface region at several different locations between the isothermal side walls. (The data shown in Fig. 4 was taken in a second apparatus, similar to the first, which measured 228 × 101 × 343 mm and had provision for off-centerline measurement of temperature and salinity.) The vertical offset of the profiles is indicative of the slight inclination of the diffusive interface. A least squares curve fit of the linear portion of these profiles indicates that the off-centerline gradients are within ±8% of the measured centerline values of 4.04°C/cm and 0.039/cm for the temperature and salinity respectively. Therefore it appears that even though the convecting region flow is very complicated, most of the diffusive region, except very near the isothermal side walls, is essentially

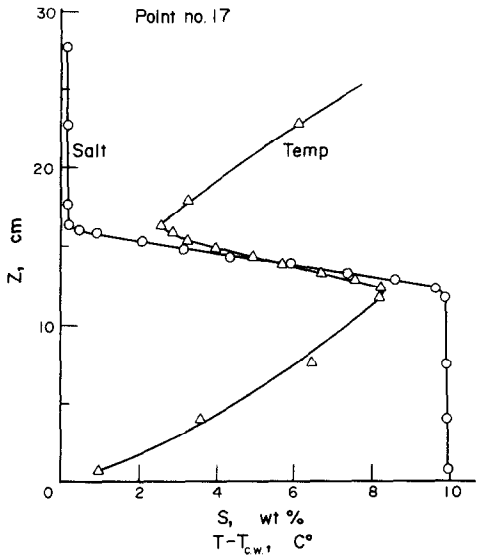

FIG. 3. Representative temperature and salinity profiles measured along vertical centerline during quasi-steady conditions.

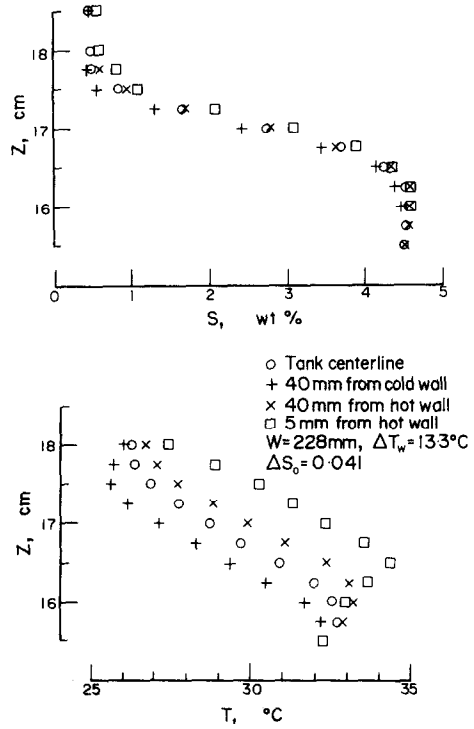

FIG. 4. Comparison of centerline and off-centerline temperature and salinity gradients measured in a diffusive interface.

one dimensional. To within experimental accuracy the temperature and salinity gradients measured on the tank centerline are representative of the total vertical flux across the diffusive interface. The salt flux is

$$F_S = -D_S \left.\frac{\partial S}{\partial Z}\right|_L \tag{1}$$

and the vertical heat flux is

$$F_T = -(\bar{\rho} c D_T) \left.\frac{\partial T}{\partial Z}\right|_L \tag{2}$$

where $\bar{\rho}$, c, D_T are the mean density, specific heat, and thermal diffusivity, and

$$\left.\frac{\partial S}{\partial Z}\right|_L \quad \text{and} \quad \left.\frac{\partial T}{\partial Z}\right|_L$$

are the linear salinity and temperature gradients measured in the interface region of thickness L respectively.

Table 1 is a summary of data collected for a total of eight separate experiments. We have omitted four data points (Nos. 4, 7, 21, 22) because of suspected miscalibration of our salinity probe. The centerline temperature and salinity gradients were determined by a least squares fit of the data points which formed the straight line portion of the measured centerline temperature and salinity profiles.

If one assumes the following constant properties:

$$\alpha \equiv \frac{1}{\bar{\rho}}\frac{\partial \rho}{\partial T} = 3 \times 10^{-4} °\mathrm{C}^{-1}$$

$$\beta \equiv \frac{1}{\bar{\rho}}\frac{\partial \rho}{\partial S} = 0.7\,\mathrm{g\ solution/g\ solute}$$

$$\nu = 0.93 \times 10^{-2}\,\mathrm{cm^2/s\ (kinematic\ viscosity)}$$

$$D_S = 1.5 \times 10^{-5}\,\mathrm{cm^2/s\ (salt\ diffusivity)}$$

$$D_T = 1.5 \times 10^{-3}\,\mathrm{cm^2/s\ (thermal\ diffusivity)}$$

which give Lewis and Prandtl numbers of 100 and 6.2 respectively, then the thermal Rayleigh number based on enclosure width, $Ra = g(\alpha \Delta T_w / \nu D_T) W^3$, for this data spans the range $2.7 \times 10^8 \leqslant Ra \leqslant 27 \times 10^8$, which for a purely homogeneous flow represents from transitional to turbulent convection. A stability number, which is a measure of the ratio of the stabilizing effect of the salinity step to the destabilizing effect of the side wall heating may be defined as $R_\rho \equiv \beta \Delta S_0 / \alpha \Delta T_w$. For the data listed in Table 1, $2.4 < R_\rho < 27.0$.

5. ANALYSIS OF RESULTS

Consider a diffusive interface bounded by two convecting regions, as in Fig. 1. Due to the wall temperature difference, heat enters the convecting region and is convected across it; the flux per unit area is given by $F_w[w/m^2]$. Heat is also transported vertically through the diffusive interface. This flux, F_T, stems from the difference in exposed isothermal wall areas of the upper and lower convecting regions in a single interface system, or from lower layer/interface systems in a multilayer system. Solute is also transported in the vertical direction [F_S in equation (1)] due to the solute difference across the diffusive interface.

For turbulent convection of a homogeneous fluid in an enclosure, the dimensionless wall flux is normally related to the driving wall temperature difference, ΔT_w, through a correlation of the form

$$Nu_w \equiv \frac{F_w W}{\Delta T_w (\rho c D_T)} = C_1 Ra^n. \tag{3}$$

The constant C_1 is empirical and $n = \frac{1}{3}$ for turbulent convection in order that the heat flux be independent

Table 1. Summary of results derived from salinity and temperature profile maps. $L_{\Delta S}$ is diffusive region thickness based on salinity profile measurements

No.	ΔT_w (°C)	ΔS_0 (g salt/ g mix.)	$\left.\frac{\partial T}{\partial Z}\right\|_L$ (°C/cm)	$\left.\frac{\partial S}{\partial Z}\right\|_L$ (cm^{-1})	$L_{\Delta S}$ (mm)
1	4.1	0.040	0.54	0.011	33.3
2	10.3	0.035	2.51	0.034	8.1
3	14.2	0.029	3.49	0.041	5.1
5	12.6	0.058	2.75	0.038	12.7
6	20.5	0.049	6.29	0.054	7.6
8	6.4	0.055	0.85	0.015	33.0
9	8.1	0.054	1.30	0.020	25.4
10	10.9	0.047	2.43	0.030	14.0
11	14.2	0.037	3.43	0.044	8.1
12	12.1	0.078	2.84	0.050	12.7
13	16.3	0.077	4.69	0.065	10.7
14	20.6	0.068	5.79	0.074	7.6
15	22.9	0.051	7.26	0.053	8.1
16	26.3	0.027	7.63	0.068	3.1
17	10.5	0.097	1.58	0.025	30.5
18	13.9	0.085	3.06	0.042	17.8
19	23.1	0.067	8.00	0.076	5.1
20	34.3	0.057	11.77	0.097	5.1
23	8.2	0.095	0.99	0.021	40.6
24	12.3	0.090	2.32	0.033	22.9
25	17.9	0.073	4.43	0.057	12.7
26	21.0	0.056	5.63	0.071	7.6
27	12.5	0.114	1.92	0.032	33.0
28	20.1	0.106	5.06	0.064	15.2
29	26.0	0.092	8.27	0.105	7.6
30	38.0	0.077	13.19	0.170	5.6
31	41.4	0.120	12.13	0.165	5.1
Estimated tolerance =	±0.5	±0.001	±10%	±0.05%	±1.0

of enclosure width. Equation (3) may be rearranged to

$$\frac{\alpha F_w}{\rho c} = C_1 \left(\frac{g D_T^2}{\nu}\right)^{\frac{1}{3}} (\alpha \Delta T_w)^{\frac{4}{3}} \tag{4}$$

where $\alpha F_w/\rho c$, (cm/s) is the apparent normalized mass flux due to the heat flux. Figure 5 is a plot of the RHS of equation (4), less the constant C_1, versus the vertical flux, $\alpha F_T/\rho c$, based on equation (2).

The shift in ordinate near 7×10^{-7} (cm/s) corresponds to a thermal Rayleigh number, $Ra \simeq 6 \times 10^8$ and is probably the result of transition, rather than turbulent flow occurring. However, it is clear from the data that

$$F_T \propto F_w \tag{5}$$

especially at $Ra > 6 \times 10^8$ where equation (4) should apply. Introducing an empirical constant in equation (5) and combining with equation (4) gives

$$\frac{\alpha F_T}{\rho c} = C_1 C_2 \left(\frac{g D_T^2}{\nu}\right)^{\frac{1}{3}} (\alpha \Delta T_w)^{\frac{4}{3}}. \tag{6}$$

Equation (6) is plotted in Fig. 5 where $C_1 C_2 = 3.4 \times 10^{-3}$.

Turner's [2] studies of a diffusive interface bounded above and below by turbulent convecting regions, and heated from below indicated that

$$\frac{\beta F_S}{\alpha F_T} = \frac{C_3}{\rho c} \tag{7}$$

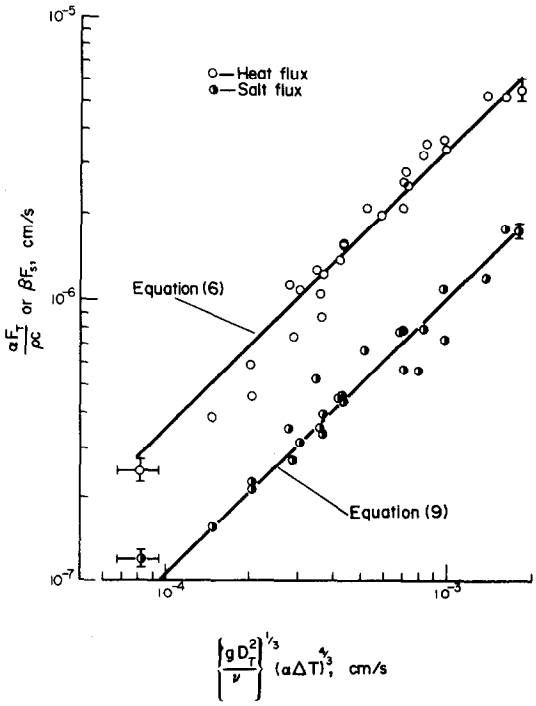

FIG. 5. Vertical fluxes through the center of the diffusive interface.

for $\beta\Delta S_0/\alpha\Delta T_0 > 2$ where ΔT_0 and ΔS_0 are the temperature and salinity differences between convecting (mixed) regions and C_3 is 0.15 based on Turner's data. Mancini's *et al.*'s [5] analysis indicated a similar result, given as

$$\frac{\beta F_S}{\alpha F_T} = f\left(\frac{\beta\Delta S_l}{\alpha\Delta T_l}\right) \tag{8}$$

where ΔS_l and ΔT_l are the salinity and temperature variations in the turbulent boundary region adjacent to the diffusive region. They found that their data was best correlated if the RHS of equation (8) was $1.5/\rho c\sqrt{(Le)}$ where $Le \simeq 100$. Thus, dependence of the vertical solute flux on the salinity variations in the turbulent boundary region must be weak. Introducing equation (7) into (6) gives

$$\beta F_S = C_1 C_2 C_3 \left\{\frac{g D_T^2}{\nu}\right\}^{\frac{1}{3}} (\alpha\Delta T_w)^{\frac{4}{3}}. \tag{9}$$

The vertical salt flux, based on equation (1) is plotted vs the RHS of equation (9) (less the constant $C_1 C_2 C_3$) in Fig. 5. The fitted curve results in $C_1 C_2 C_3 = 1.0 \times 10^{-3}$ in equation (9) and $C_3 \simeq 0.29$ by comparison with the result obtained for equation (6).

The validity of equation (9) may be tested by recognizing that

$$\left.\frac{\partial S}{\partial Z}\right|_L = \frac{\Delta S_L}{L} \tag{10}$$

where ΔS_L is the measured change in solute over the linear portion of the solute profile shown in Fig. 3 and L is the observed diffusive interface thickness. Combining (10) with (9) and (1) and assuming that $\Delta S_L \propto \Delta S_0$ results in

$$L \propto \left[\frac{g}{\nu D_T}\right]^{-\frac{1}{3}} Le^{-1} \frac{\beta\Delta S_0}{(\alpha\Delta T_w)^{\frac{4}{3}}}. \tag{11}$$

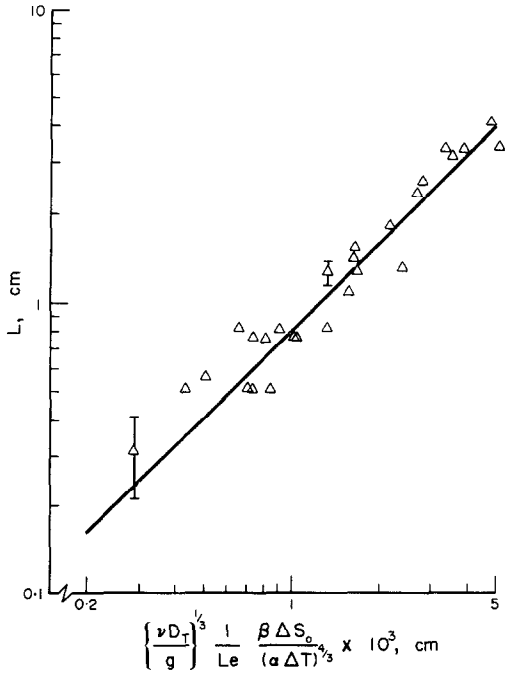

FIG. 6. Measured diffusive interface thickness.

The measured values of L (mm) are plotted against the RHS of (11) in Fig. 6 where it is seen that the functional dependence indicated in equation (11) fits the data well over a two order of magnitude variation in abscissa.

6. EXTENSION OF RESULTS TO MULTILAYERED SYSTEMS

Consider a stratified fluid with state equation given by

$$\rho = \bar{\rho}\{1-\alpha(T-\bar{T})+\beta(S-\bar{S})\} \tag{12}$$

which is contained in a tall slot of height H. The fluid initially has linear stratification such that its density is given by

$$\rho = \bar{\rho}\left\{1-\frac{B^2}{g}Z\right\} \tag{13}$$

where

$$B = \left(-\frac{g}{\bar{\rho}}\frac{\partial\rho}{\partial Z}\right)^{\frac{1}{2}}\Bigg|_{t=0}$$

is the Brunt–Väisälä frequency. The linear density stratification results from a salinity gradient

$$\left.\frac{\partial S}{\partial Z}\right|_{t=0} = -\frac{B^2}{g\beta} \tag{14}$$

and vertical solute flux in the absence of fluid motion is by diffusion, given by

$$\beta F_S(0) = \frac{S(0)-S(H)}{\frac{H}{\beta D_S}} = D_S\frac{B^2}{g} \tag{15}$$

where $H/\beta D_S$ is the resistance to solute flux analogous to the thermal resistance encountered in one-dimensional conduction heat transfer analysis.

It has been previously shown that if the above system is exposed to a supercritical lateral temperature gradient due to a sufficiently large wall temperature difference, layers will form in the fluid, contained in a slot of width W, as shown schematically in Fig. 7 [4–9]. The flow in each convecting layer is clockwise. Once established, the convecting layers are well mixed, of height h, and separated by diffusive interfaces of thickness L. The resulting step-like density structure is sketched in the figure. Numerical stability theory [6], and laboratory experimentation [5], have demonstrated that layers will form spontaneously when the Rayleigh number

$$R \equiv \frac{g\alpha\Delta T_w}{\nu D_T}\bar{h}^3 \geqslant 15\,000 \tag{16}$$

where $\bar{h} \equiv g\alpha\Delta T_w/B^2$ is the correct length scale when $W \gg \bar{h}$. In this case the initial layer thickness has been found to be $\simeq 0.6\bar{h}$ [5, 6]. However, the layers successively merge, two for one, on a time scale which is on the order of $\bar{h}^2/D_T$, [19]. Thus a region of height H containing approximately 20 convecting layers would at some later time contain approximately 10 layers, each with double their former thickness.

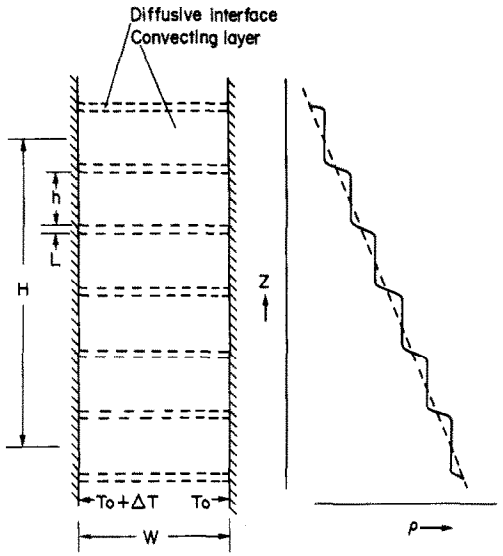

FIG. 7. Schematic of layered convection in a slot. The fluid initially has linear stratification. At supercritical conditions, layers spontaneously form, producing the step-like density profile shown.

We wish to ascertain how the presence of the layers effects the vertical flux of heat and salt. Furthermore, how are the vertical fluxes effected by the successive merging of layers? Our analysis of a single interface bounded above and below by turbulent convecting regions may be used to this end.

The vertical solute flux through a series of $N+1$ well mixed convecting layers separated by N diffusive interfaces is given by

$$\beta F_S(N) = \frac{S(0)-S(H)}{\sum_{i=1}^{N} r_i} \tag{17}$$

where comparison with equation (9) indicates that the resistance per interface, r_i is

$$r_i = \frac{1}{C_1 C_2 C_3}\left\{\frac{gD_T^2}{\nu}\right\}^{-\frac{1}{3}}\frac{(\beta\Delta S_0)_i}{(\alpha\Delta T_w)^{\frac{4}{3}}} \tag{18}$$

where $(\Delta S_0)_i$ is the solute concentration change across the ith diffusive interface. Performing the summation indicated in equation (17) and noting that

$$\sum_{i=1}^{N}(\Delta S_0)_i = S(0)-S(H)$$

results in

$$\frac{\beta F_S(N)}{\beta F_S(0)} = C_1 C_2 C_3 Le R^{\frac{1}{3}} \tag{19}$$

where $Le \equiv D_T/D_S$ is the Lewis number. Since R remains constant this result indicates that the vertical solute flux is uneffected by the number of layers present at a given time. Once convective layers form, the vertical flux is amplified over the purely diffusive condition by a factor proportional to $\Delta T_w^{\frac{4}{3}}$; however as the layer merging proceeds the vertical solute flux, and hence the vertical heat flux from equation (7), are unmodified as long as a multi-layer system exists.

Furthermore, as a layered system evolves, with adjacent layers merging to form new convective layers of thickness $2h$, the thickness of the diffusive interface separating layers must also double, in order to maintain a constant vertical solute flux. This indicates that there must be some form of similarity to the flow where the relative proportions of a convective layer are fixed by the initial stratification of the fluid.

7. CONCLUSIONS

We have investigated the vertical transport across a diffusive interface, bounded above and below by turbulent convecting regions, and found that the vertical fluxes are given by equations (6) and (9) over the range of variables tested. We have also found that the ratio of fluxes is a constant given by equation (7) with C_3 experimentally determined to be $\simeq 0.29$ for $Ra > 6 \times 10^8$. This is compared with a value of $C_3 = 0.15$ empirically determined by Turner [2] for the similar case of a diffusive interface which is heated from below. Our experiments differ from Turner's in that the turbulent convecting regions in the present experiments had some mean lateral motion driven by the side wall temperature difference, superimposed upon the turbulence in the convecting region; whereas Turner's experiments (and those reported by Mancini *et al.* [3]) did not. In both cases it appears that the mechanism for controling the thickness of the diffusive region, L, and hence the flux through it, is the same.

In the present work, the characteristics of the turbulent convection were not measured directly. Instead, we measured the imposed wall temperature difference and used it as a yardstick on the intensity of the flow in a fixed size enclosure. The wall heat flux, F_w, and hence the kinetic energy of the flow in the convecting region, is proportional to $(\alpha\Delta T_w)^{\frac{4}{3}}$. This mechanical energy continually limits the thickness of the diffusive region through viscous shear at its boundaries. As the thickness decreases [note equation (11)] the gradient through the interface, and hence the flux through this region, must increase by the same factor, $(\alpha\Delta T_w)^{\frac{4}{3}}$. Mancini *et al.* [3] found the same form of interface thickness and vertical flux dependence in their experiments. It might be that the value of the empirical constants which we have developed, C_1, C_2, C_3 would change if data were collected in a different sized apparatus. However, the functional dependence of the fluxes on the controling parameters, and hence the conclusions reached as a result of equation (19) would be expected to hold.

When applied to a multi-layered system, these "flux laws" result in the conclusion that the vertical flux is independent of the number and size of layers existing over a given height H except for possible variations in C_1, C_2, and C_3. For a steadily applied lateral temperature gradient, the vertical flux is constant and given by equation (19). As adjacent layers merge, the doubling in convecting region height, h, is accompanied by a doubling in diffusive region thickness, L, in order to maintain this constant flux.

Acknowledgement—Funding for this research came partly from the NSF Research Initiation Program under grant GK 37396, and partly from the Research Division of Clarkson College of Technology. This support is gratefully acknowledged.

REFERENCES

1. J. S. Turner, Double-diffusive phenomena, *Ann. Rev. Fluid Mech.* **6**, 37–56 (1974).
2. J. S. Turner, The coupled turbulent transports of salt and heat across a sharp density interface, *Int. J. Heat Mass Transfer* **8**, 759–767 (1965).
3. T. R. Mancini, R. I. Loehrke and R. D. Haberstroh, Heat and mass transfer in layered natural convection, ASME Paper 74-HT-41 (1974).
4. J. A. Thrope, P. K. Hutt and R. Soulsby, The effect of horizontal gradients on thermohaline convection, *J. Fluid Mech.* **38**, 375–400 (1969).
5. C. F. Chen, D. G. Briggs and R. A. Wirtz, Stability of thermal convection in a salinity gradient due to lateral heating, *Int. J. Heat Mass Transfer* **14**, 57–65 (1971).
6. C. F. Chen, Onset of cellular convection in a salinity Gradient due to a lateral temperature gradient, *J. Fluid Mech.* **63**, 563–576 (1974).
7. L. H. Liu, Numerical simulation of convective layer formation in a slot, MIE report No. 004, MIE Department, Clarkson College of Technology, Potsdam, New York (1974).
8. J. E. Hart, On sideways diffusive instability, *J. Fluid Mech.* **49**, 279–288 (1971).
9. J. E. Hart, Finite amplitude sideways diffusive convection, *J. Fluid Mech.* **59**, 47–64 (1973).
10. J. S. Turner and C. F. Chen, Two-dimensional effects in double-diffusive convection, *J. Fluid Mech.* **63**, 577–592 (1974).
11. R. I. Tait and M. R. Howe, Some observations of thermohaline stratification in the deep ocean, *Deep-Sea Res.* **15**, 275–280 (1968).
12. V. T. Neal, S. Neshyba and W. Denner, Thermal stratification in the Arctic Ocean, *Science* **166**, 373–374 (1969).
13. R. A. Hoare, Problems of heat transfer in Lake Vanada, a density stratified antarctic lake, *Nature, Lond.* **210**, 787–789 (1966).
14. H. Stommel and K. N. Fedorov, Small scale structure in temperature and salinity near Timor and Mundanao, *Tellus* **19**, 306–325 (1967).
15. J. W. Cooper and H. Stommel, Regularly spaced steps in the main thermocline near Bermuda, *J. Geophys. Res.* **73**, 5849–5854 (1968).
16. E. T. Degens and D. A. Ross, The Red Sea hot brines, *Scient. Am.* **222**(4), 32–53 (1970).
17. J. S. Turner, *Buoyancy Effects in Fluids*. Cambridge Univ. Press, Cambridge (1973).
18. D. T. Hurle and E. Jackeman, Soret driven thermosolutal convection, *J. Fluid Mech.* **47**, 667–687 (1971).
19. R. A. Wirtz, D. G. Briggs and C. F. Chen, Physical and numerical experiments on layered convection in a density stratified fluid, *Geophys. Fluid Dynam.* **3**, 265–288 (1972).

TRANSPORT DE CHALEUR ET DE MASSE A TRAVERS UN INTERFACE DIFFUSIF ENTRE DES ZONES DE CONVECTION TURBULENTES

Résumé—On étudie expérimentalement le transport vertical de la chaleur et d'un soluté, à travers un interface diffusif stable séparant deux zones de convection turbulentes de concentrations différentes. Dans ce cas la convection est entrainée par un chauffage latéral tel que l'interface horizontal séparant les régions convectrices soit compris entre deux couches limites en mouvements opposés. Des lois sont formulées pour les flux de transport vertical de chaleur et de masse. Ces lois sont ensuite utilisées afin d'étudier l'effet sur le transport vertical dans les systèmes convectifs à plusieurs couches du changement de la dimension et du nombre des couches. Il apparait que dans de tels systèmes le transport vertical est indépendant de la dimension des couches convectrices et de leur nombre.

WÄRME- UND STOFFTRANSPORT AN DIFFUSEN, VON TURBULENTEN KONVEKTIONSBEREICHEN BEGRENZTEN TRENNFLÄCHEN

Zusammenfassung—Der vertikale Wärme- und Stofftransport über eine stabile diffuse Zwischenschicht zwischen zwei turbulenten Konvektionsbereichen von unterschiedlicher Konzentration wird experimentell untersucht. Die Konvektion wird hier durch seitliche Beheizung hervorgerufen, so daß die horizontale Zwischenschicht, die die Konvektionsbereiche trennt, zwischen zwei in entgegengesetzter Richtung fließende turbulente Grenzschichten eingeschlossen ist. Für den senkrechten Wärme- und Stofftransport werden Gesetze für die Stromdichten entwickelt. Diese Gesetze dienen dazu, den Einfluß von Schichtgröße und Schichtanzahl auf den senkrechten Transport in Vielschichten-Konvektionssystemen zu untersuchen. Es ergab sich, daß der Senkrecht-Transport in solchen Systemen unabhängig ist von der Größe und der Anzahl der Konvektionsschichten.

ПЕРЕНОС ТЕПЛА И МАССЫ ПОПЕРЕК ДИФФУЗНЫХ ПОВЕРХНОСТЕЙ РАЗДЕЛА, ОГРАНИЧЕННЫХ ТУРБУЛЕНТНЫМИ КОНВЕКТИВНЫМИ ОБЛАСТЯМИ

Аннотация — Проведено экспериментальное исследование вертикального переноса тепла и растворенного вещества поперек устойчивой диффузионной поверхности раздела, ограниченной двумя турбулентными конвективными областями различной концентрации. Конвекция в этом сулчае создается боковым нагревом таким образом, что горизонтальная поверхность, разделяющая конвективные зоны, располагается между двумя противоположно направленными турбулентными пограничными слоями. Получены закономерности для потоков при вертикальном переносе тепла и растворенного вещества. Далее эти соотношения используются для исследования влияния изменения размера и числа слоев на вертикальный перенос в многослойных конвективных системах. Найдено, что вертикальный перенос в таких системах не зависит от размера или числа конвективных слоев.